CORRESPONDENCE BETWEEN SOLAR FINE-SCALE STRUCTURES IN THE CORONA, TRANSITION REGION, AND LOWER ATMOSPHERE FROM COLLABORATIVE OBSERVATIONS

D. Moses, J.W. Cook, J.-D.F. Bartoe, G.E. Brueckner, K.P. Dere, D.F. Webb, J.M. Davis, F. Recely, S.F. Martin, H. Zirin

For submission to THE ASTROPHYSICAL JOURNAL

September 1989

ABSTRACT

The American Science and Engineering Soft X-Ray Imaging Payload and the Naval Research Laboratory High Resolution Telescope and Spectrograph (HRTS) instrument were launched from White Sands on 11 December 1987 in coordinated sounding rocket flights to investigate the correspondence of coronal and transition region structures, especially the relationship between X-ray bright points (XBPs) and transition region small spatial scale energetic events. We present the coaligned data from X-ray images, maps of sites of transition region energetic events observed in C IV (100,000 K), HRTS 1600 A spectroheliograms of the T_{min} region and ground-based magnetogram and He I 10830 A images.

The transition region energetic events do not correspond to XBPs; in fact, they are associated with X-ray dark lanes in quiet regions. XBPs are associated with magnetic dipoles often appearing as prominent network elements, and the actual corresponding features in C IV observations are brighter, larger scale (20 arc sec) regions of complex velocity flows of order 40 km s^{-1}. However, analogously as He I 10830 A dark points are not uniquely associated with XBPs, so also there are other similar C IV features which do correspond to an XBP in the X-ray image.

The C IV energetic events appear to be concentrated in the quiet Sun at the edges of strong network, or in weaker network regions. The X-ray image shows a pattern of dark lanes in quiet Sun areas, and the C IV events are predominantly concentrated within these dark lanes, avoiding areas of hazy, slightly brighter X-ray emission probably corresponding to unresolved loop systems seen even in quiet areas of the disk. We also find a greater number of C IV events than we would have expected from the results of a disk survey undertaken on the Spacelab 2 flight of the HRTS payload (Cook et al. 1987). This is possibly because

of the occurrence of particularly rich regions (associated with the X-ray dark lanes) in the field of view, and by an extended detection threshold from better spatial resolution with the HRTS V data.

I. INTRODUCTION

Fine scale features have been observed in the upper solar atmosphere both in the corona and in the transition region. X-ray bright points (XBPs), structures at the 10-20 arc sec spatial scale, lasting the order of 12 hours but with more transient periods of activity, have been observed from space by soft X-ray instruments viewing the corona. EUV spectrographs viewing transition region and chromospheric plasmas have observed highly transient fine scale structures down to arc second spatial scales. In particular, small scale (2 arc sec) features in transition region emission lines such as C IV 1548 A and 1550 A have been observed which show line profiles broadened to the red or blue by 50-200 km s^{-1} with average lifetimes of the order of 90 s or less (Brueckner and Bartoe 1983; Cook et al. 1987). We wanted to know if these C IV energetic events are related to XBPs, but the lack of near simultaneous X-ray and EUV observations left the correspondence between these coronal and transition region fine-scale transient structures unclear. In addition, we would like to know how these features are associated with lower atmospheric structures, for example, with magnetic field structures and with possible He I 10830 A counterparts.

In an effort to determine this correspondence, a collaborative "bright point campaign" of co-observations from ground and space was organized whose primary purpose was to determine the relationship of X-ray bright points, HRTS high velocity transition region energetic events, He I 10830 A dark points or other structures, and photospheric magnetic structures. Coordinated sounding rocket flights were made by the American Science and Engineering (AS&E) High Resolution Soft X-Ray Imaging Payload and the Naval Research Laboratory (NRL) High Resolution Telescope and Spectrograph (HRTS) experiment from White Sands

on 1987 December 11, with launches at 1815 UT (AS&E) and 1845 UT (NRL). The AS&E experiment obtained full disk coronal images over the wavelength range 8-64 A, emitted by 10^6 K plasmas, with a spatial resolution of approximately 2 arc sec. The HRTS spectrograph slit of 920 arc sec length was rastered in 2 arc sec steps across an approximately 3 arc min wide area in the northeast quadrant, covering a quiet area out to the solar limb. HRTS spectra were obtained of the C IV 1548 A and 1550 A lines, emitted by transition region plasmas at 10^5 K. In addition, spectroheliograms covering an area of approximately 920 x 460 arc sec were taken over a 20 A passband centered at 1600 A.

Collaborative ground based observations were also obtained, including magnetograms (NSO/Kitt Peak and BBSO), He I 10830 A (NSO/Kitt Peak), and H-alpha (BBSO). The HRTS spectroheliograms can be accurately registered with the magnetograms. The slit position of HRTS spectrograms covering the transition region C IV lines 1548 A and 1550 A can be accurately placed on the HRTS spectroheliograms. We then studied the correlation of sites of small spatial scale (2 arc sec) high velocity (100 km s^{-1}) transition region energetic events with the ground based data, and in particular the spatial relationship with the quiet Sun network.

In this paper we will present the co-registered observations from the two sounding rocket experiments and the ground-based observations, and discuss their correspondence and interpretation.

II. ROCKET INSTRUMENTATION

In this section we describe the two rocket payload experiments of the bright point collaboration.

(i) AS&E X-ray payload

The American Science and Engineering High Resolution Soft X-Ray Solar Astronomy Imaging Payload was flown on 15 August 1987 and 11 December 1987 in participation with the Collaborative Bright Point Campaign. X-ray imaging is achieved in the AS&E payload by grazing incidence optics. The AS&E payload was programmed to reconfigure the X-ray telescope during flight from an instrument based on a photographic film detector obtaining full disk images to an instrument based on an X-ray sensitive CCD camera obtaining 2 arc min x 2 arc min images. Only the full disk X-ray photographic images presented in Figure 1 are used in the collaborative Bright Point Campaign.

The primary mirror is a Wolter Schwarzschild design with principal diameter of 30.48 cm and focal length of 144.9 cm. The reflecting surfaces of the mirror are uncoated fused silica. The level of suppression of scattering which is obtained with this mirror material by the reduction in surface roughness results in a point spread function relatively independent of wavelength (particularly in comparison to the Kanigen Skylab S-054 and sounding rocket mirrors). However, the reflectivity of this surface at the grazing angles of this mirror (approximately 1.5 degrees) is strongly wavelength dependent and defines the decline of the short wavelength response of the system below 30 angstroms.

Kodak SO-212 film was chosen as the primary photographic film for this mission because of its superior sensitivity with the longer wavelength filter used to image the "cooler" coronal plasma typical of X-ray bright points. The resolution of the combination of the telescope optics and the SO-212 film is

limited by the film but is comparable to the practical level of microdensitometry which results in pixels of 3 arc sec x 3 arc sec. This film was manufactured in 1973 for the Skylab S-054 X-Ray Spectrographic Telescope Experiment Program and has since been kept in cold storage. Aging of the film has had little impact on its X-ray response and advances in the photometric process continue to make this film a valuable resource for X-ray imaging (Moses et al. 1989). Since this film has been used for almost all high resolution X-ray photographic imaging of the solar corona, comparison with prior observations in synoptic studies is greatly facilitated.

In addition to the filtering effect of the reflectivity of the imaging mirror, the X-rays are also filtered by a heat rejection prefilter of approximately 1500 Angstroms of Aluminum and one of two focal plane filters: (1) a 17.5 micron thick Beryllium filter with a bandpass of 8 to 20 Angstroms or (2) a 1 micron thick polypropylene filter coated by 2000 Angstroms of Aluminum (for visible light rejection) with a dual bandpass of 8 to 39 and 44 to 64 Angstroms. A series of exposures through each of these filters was made with exposure times of 1/2 sec, 1 sec, 3 sec, 9 sec and 30 sec. This sequence was chosen to accommodate the dynamic range of the coronal X-ray emission (which can vary from 10^3 for quiet sun to more than 10^6 for a flare) as well as provide additional control on variations induced by photographic development (Moses et al., 1989). The X-ray throughput of the instrument with the polypropylene filter is greater than with the Beryllium filter for all temperatures of X-ray emitting plasmas. Furthermore, the throughput of the polypropylene filter is proportionally much greater for low temperature plasma so that the ratio of flux through the polypropylene filter to the flux through the Beryl-

lium filter provides a good plasma temperature diagnostic over the range of 1 x 10^6K to 2 x 10^7K (Vaiana, Krieger and Timothy, 1973). Since the objective of the collaborative observations is small scale coronal structure and since such structures are typically cool (1.5 - 1.8 x 10^6K), the primary X-ray data used in the correspondence studies are the longest available exposures through polypropylene filters which are shown in Figure 1.

The Collaborative Bright Point Campaign had been attempted previously in August 1985 during the Spacelab 2 flight of the HRTS instrument. The Collaborative AS&E Sounding Rocket Flight was aborted during boost phase by the White Sands Missile Range Safety Officer. Beyond creating the necessity of repeating the Collaborative in 1987 from two sequentially launched rocket platforms, this abort also left the legacy of a contamination coating on the X-ray mirror from the explosives used to destroy the rocket booster. An effort toward cleaning the mirror was made before the August 1987 flight. A review of the image from the August flight compared with previous coronal images compelled us to attempt a more invasive cleaning effort.

The second X-ray mirror cleaning effort was conducted with a considerably more vigorous scrubbing action coupled with particular attention to removing organic deposits during the final sequence of solvent rinses. This cleaning effort was a dramatic success and the resulting images from the December 1987 flight show details as fine as any soft X-ray image of the solar corona. As a precaution, an extra 60-second exposure through the thinnest available polypropylene filter was added to the December 1987 flight exposure sequence. With the added integration time obtained with the 60 sec exposure, the threshold

emission measure ($\int N_e^2$ dl) for detection of 1.6 x 10^6K plasma typical of small scale coronal structure became 1.2 x 10^{25} cm^5. Furthermore, the contrast of the December 1987 image was improved to the extent that dark lanes between regions of diffuse, quiet coronal emission became readily apparent. These dark lanes are not associated with filament channels, neutral lines, or any other readily perceivable magnetic structure. While these features can be found on review of some previous X-ray coronal images, they do not appear as distinctly defined. It is reasonable to conclude that the intrinsic improvement in image contrast of the fused silica mirror over previous metal mirrors coupled with the reduction in scatter by contaminants removed by the cleaning has resulted in the recognition of a coronal feature which, as will be discussed in Section IV, shows a unique relationship with fine scale transition region energetic events.

(ii) The NRL HRTS experiment

The High Resolution Telescope and Spectrograph (HRTS) instrument was flown as a rocket payload for the fifth time on 11 December 1987. HRTS consists of a 30 cm cassegrain telescope, a broadband spectroheliograph which was tuned to a wavelength region around 1600 A, a stigmatic slit spectrograph which covered a wavelength range from 1520-1570 A which included the C IV lines at 1548 A and 1550 A, and an H-alpha imaging system. The spatial resolution of the instrument is potentially sub arc second, and in this flight the smallest resolved spatial features in the slit spectrograph and the spectroheliograph are approximately 1 arc sec in size. Slit spectra were recorded by film exposure using Kodak type 101 emulsion, and spectroheliograph images on Kodak type 104 emulsion. The spectrograph slit length of 920 arc sec was rastered in 1 or 2 arc

sec steps across an approximately 3 arc min wide area in the northeast quadrant, covering a quiet area out to the solar limb. In addition, spectroheliograms covering a field of 920 x 460 arc sec were taken every other raster step of the slit spectrograph.

An example of a spectroheliograph exposure can be seen in Figure 2. The spectroheliograph passband is centered at 1600 A, with a 20 A FWHM. The predominant flux source in this passband is the ultraviolet continuum, arising from the solar temperature minimum region (see Vernazza et al. 1976), with remaining flux contributed by chromospheric and transition region emission lines. From an integration of this passband over a representative quiet solar spectrum from the atlas of Kjeldseth Moe et al. (1976), where we have estimated the continuum level and separated the flux into emission line and continuum contributions, we find that 72% of the flux from this quiet region would arise from continuum emission if observed by the HRTS spectroheliograph. The spectroheliograph field of view is 7.5 x 15 arc min in size. The HRTS spectrograph slit passes down the approximate center of the spectroheliograph image, which is obtained from a solar image reflected from the mirrored slit jaw plates. Three fiducial wires cross the image field perpendicular to the slit.

A series of film exposures of length 2.0 s, 1.0 s, and 0.5 s was taken at every other raster step of the slit spectrograph. In practice, the longest 2.0 s exposures have been used. After initially developing a flight film sample, it was clear that the spectroheliograph instrumental efficiency was down by as much as a factor of 10. With the help of Brian Dohne, a chemical developer was devised which optimally brought out the film latent image, effectively boosting the tail and steepening the gamma of the film characteristic curve. Although

the developed images had a greater fog level than nominal, the final images were usable and photometrically reliable.

The slit spectrograph on this flight covered the 1520-1570 A wavelength range. The slit was widened to a 1 arc sec width to bring down the exposure time and allow more exposures, covering a greater surface area. The resulting spectral resolution was 0.10 A. This region contains chromospheric lines of Si I, Si II, C I, Fe I, and other species, and the transition region resonance lines of C IV at 1548 A and 1550 A; in addition, the continuum in this region arises from the temperature minimum region of the solar atmosphere. In this paper we discuss only the C IV slit spectrograph observations. An exposure time of 2.4 s was used for the raster exposures, which optimally exposed the C IV lines.

The slit spectrograph was rastered across the solar field by mechanically stepping the slit position. We wanted to raster as wide an area as possible, but with steps small enough not to miss C IV turbulent events in the field. From the size distribution for these events given in Cook et al. (1987), a step size of 2 arc sec was generally used, although one raster with 1 arc sec step size was performed. As noted above, a spectroheliograph exposure was taken with every second raster step. On these spectroheliograph images the slit can be seen displaced in the raster direction in successive images. Although it is possible to raster over larger fields, optical aberrations in the slit spectrograph increase beyond a distance of approximately 30 arc sec to left or right of the slit central position, and to cover a wide field four individual rasters were made, with the telescope pointing changed between rasters so that no individual raster exceeded 25 arc sec relative to the central slit position. The nominal raster layout was to have 4 individual rasters of the 920 arc sec long

slit in the following pattern: raster 1 (2 arc sec steps, 26 position); 5 arc sec inter-raster spacing; raster 2 (1 arc sec steps, 21 positions); 5 arc sec inter-raster spacing; raster 3 (2 arc sec steps, 26 positions); 10 arc sec inter-raster spacing; raster 4 (2 arc sec steps, 24 positions). The total width of the pattern is nominally 186 arc sec, or 3 arc min.

III. THE COLLABORATIVE BRIGHT POINT CAMPAIGN

The collaborative observing plan called for a morning launch of the AS&E payload, followed in one-half hour by the NRL HRTS payload, both on Black Brant IX sounding rockets. In an effort to minimize possible launch constraints which might make it harder to launch two closely timed rockets, each Black Brant was equipped with a Saab S-19 boost phase guidance system. The S-19 allows a wider tolerance for high altitude winds, and gives a lower dispersion in the re-entry trajectory and final landing spot of the rocket and payload. The morning launch time was chosen to allow ground-based observations at Kitt Peak and Big Bear Solar Observatory (BBSO) to begin an hour or more before launch, while still keeping the actual flight within a time period which would typically insure good seeing at the ground-based observing sites. Observing programs at the ground-based sites were developed which emphasized He I 10830 A images and magnetograms from Kitt Peak, and videomagnetograms and H-alpha from Big Bear. At Kitt Peak, full disk images were taken outside the actual flight period, while during the flight period a 512 x 256 arc sec field at the planned position of the HRTS field was viewed in He I 10830 A. At Big Bear, a program was devised where videomagnetograms and film H-alpha images were taken during the observing day in overlapped boxes which also covered the planned HRTS field, while other areas of the Sun where magnetograms showed bipolar regions

were also occasionally observed to further support the full disk field of the AS&E X-ray payload.

This planned program was actually attempted several times during the summer of 1987, but was unsuccessful because of difficulties in launching the first rocket because of malfunctions with the S-19 rocket guidance system. On 1987 August 15 the AS&E rocket was successfully launched, but one-half hour later the NRL rocket could not be launched because of a similar S-19 malfunction. The X-ray and ground-based data obtained on 1987 August 15 are not discussed in this paper.

Finally on 1987 December 15 both rockets were successfully launched. This time, however, another malfunction occurred which affected the pointing of the HRTS payload. Pointing information on pitch, roll, and yaw for the Lockheed SPARCS payload pointing system was uplinked by radio to the rocket after launch, and a data dropout occurred during the sending of the roll angle. Instead of the desired pointing at the southwest quadrant, covering an area including an active region at the limb, the roll received put the pointing almost 180` away, in the northeast quadrant, with HRTS observing one of the quietest areas on the disk.

[The actually desired southwest limb pointing was jointly observed by participants in the Coronal Magnetic Structures Observing Campaign (COMSTOC), and a broad additional range of data is available for his pointing. The full disk X-ray images, and the small field CCD X-ray images of this area, will be useful in a separate COMSTOC analysis.]

IV. COALIGNMENT OF THE OBSERVATIONAL MATERIAL

We have coaligned the three full disk images which were obtained: the full disk Kitt Peak magnetogram and He I 10830 A, and the X-ray image. We have processed digitized full disk data which were obtained hours before and after the rocket flights by compute to produce a rotated image for the time of flight. This is a computer constructed image in which each pixel in the constructed image is obtained by rotating that pixel position to the time of the actual full disk observation, using the full geometry of the tilted solar axis and a formula for solar differential rotation. This rotated pixel position falls on the actual image, and its numerical value is taken as a linearly weighted average of the (typically four) original observed pixels which contribute to it. Solar rotation near the disk center is 9 arc sec an hour, and in comparing observations hours apart, as we have, where we are trying to determine correspondences in features which may be only arc seconds in dimension (the C IV high velocity events, for example), solar rotation is a significant effect. This is purely a geometrical correction, and does not account for actual temporal evolution of features between the time of the actual observation and the time of the calculated rotated image. In addition, no attempt is made to further adjust the numerical value of this constructed pixel for the changed line of sight, so for example a constructed pixel in a magnetogram can have a magnetic field value from an area of the actual observed magnetogram eastward or westward of this position, with a different line of sight angle, or a He I 10830 A constructed image can have constructed pixel values which are not corrected for changed limb brightening coefficient at the new constructed pixel position.

The Kitt Peak magnetogram and He I 10830 A images are obtained at different wavelengths by the same instrument, and are at the same scale, nominally 1 arc sec per pixel; in addition, no rotation should be necessary in coaligning different images. After placing all Kitt Peak full disk images at the same center image coordinates, we compared magnetograms and He I images. In the Kitt Peak gray scale image display representation most often seen, the He I image is surrounded by a white ring at the limb, which is actually limb brightening in this chromospheric line at a numerical intensity which is represented by white in the gray scale used. As a check, we verified that the magnetogram limb falls at the inside of this white band on the He I image, as should the limb from a photospheric line.

The general problem of coaligning images from different instruments can be difficult. Besides the obvious necessity to place the two images on a similar linear scale and rotational orientation, there are often instrumental aberrations present so that to some extent the image is not flat field, perhaps in a nonlinear barrel sense. We have developed a general computer program to align two images where a number of corresponding points on each are believed to exist. This program constructs a rescaled, rotated image from one of the original images which in a least squares sense produces the best coalignment of the selected pairs of fiducial points on each original image. The rescaling can be either linear or nonlinear in x and y.

We coaligned the full disk X-ray image using this program, where as fiducial points we took XBPs and their plausible He I dark point counterparts, or other pairs of fiducial features are small spatial scale which appeared to be plausible counterparts. Although subjective to some extent, this was very straightforward to accomplish. We then checked the resulting aligned X-ray

image's limb with the limbs of the Kitt Peak He I and magnetogram images. The X-ray limb, black where silhouetted against the brighter general off disk coronal emission, fell at the magnetogram limb and the inside of the limb brightening ring at the He I limb. As a further check, we compared the full disk white light image also obtained by the AS&E experiment with the X-ray image and found that the white light and dark X-ray limb were coincident.

V. RESULTS FROM THE COALIGNED DATA

The XBPs observed are associated with magnetic dipoles in the magnetograms, and with dark points in the He I 10830 A data. However, every magnetic dipole, and every dark point, are not always associated with a corresponding XBP. Webb and Moses (1989) studied the X-ray and Big Bear videomagnetogram data from the December 11 and August 15 launch efforts in an attempt to classify the nature of the magnetic bipolar regions associated with XBPs. In quiet network regions magnetic flux appears to emerge in small bipolar ephemeral regions, spread apart with time, and disappear either by gradual fading of the two opposite polarity elements of the ephemeral region or by cancellation of one element with another existing opposite polarity element with its own previous evolution as an internetwork element, active region remnant, or ephemeral region (see Martin and Harvey 1979). A time series of magnetograph observations over several hours is necessary to classify a magnetic bipolar region observed in a snapshot observation as either an emerging flux ephemeral region, a disappearing flux cancellation, or a stationary flux element lasting an appreciable time, perhaps simply fading with time. Because of excellent temporal coverage, Webb and Moses (1989) were able to characterize the magnetic dipoles corresponding to XBPs as emerging, stationary, or disappearing flux, and found that

the most significant class of magnetic dipole signature was disappearing flux regions.

We do not have comparable temporal coverage in the HRTS field of observation. The roll error in the HRTS V pointing described in Section III oriented the HRTS field of view completely outside of the target 10 arc min x 25 arc min region of observation for the Big Bear videomagnetogram. The temporal resolution of the Kitt Peak full disk magnetograms is sufficient to show the magnetic development of some XBPs as shown in Fig. 2.

We have studied the identification in the combined data of sites corresponding to locations in HRTS spectra of the C IV 1550 A wavelength region showing the high-velocity energetic events described before. The method is to coalign HRTS V spectroheliograms, which image a wavelength interval around 1600 A where flux is emitted predominantly from the temperature minimum continuum, with ground-based magnetograms. The T_{min} images are known (see Cook, Brueckner, and Bartoe 1983) to be highly correlated in their fine structure with magnetograms, and in fact we can coalign the HRTS spectroheliograms to the Kitt Peak magnetogram to around 5 arc sec accuracy. The HRTS spectrograph slit can be seen on the HRTS spectroheliograph images, and thus the location of transition region C IV energetic events from the spectra can be accurately transferred to the spectroheliograms, and thus to the magnetograms and the ground-based data.

We have measured the location of the energetic events observed in C IV from HRTS slit spectrograph data. These events appear to be located at the edges of strong field network elements, or even within network elements of weakest magnetic field; they appear to generally avoid areas away from networks such as cell centers completely. The C IV events are not X-ray bright points, which

instead occur at sites of magnetic dipoles whose corresponding features in the HRTS C IV data are larger and more intense areas instead of the small high-velocity energetic events.

In Figure 2 the HRTS data has been aligned and compared with the X-ray, magnetograph, and He I 10830 A data. An original goal of the bright point campaign was to determine the correspondence of the transition region high velocity events seen in C IV with the observations from lower atmospheric regions and with coronal XBPs. The transition region high velocity events appear to be concentrated at the edges of strong network, or in weaker network regions, in the quiet Sun. They are not the transition region counterparts of XBPs. The X-ray image shows a pattern of dark lanes in quiet Sun areas, and the C IV events appear to be predominantly concentrated within these dark lanes, avoiding areas of hazy brighter X-ray emission probably corresponding to unresolved loop systems in active region areas of the disk.

We have been unable to determine if the individual C IV events are associated with magnetic dipoles, as are the XBPs, although it is clear that such an association, if it exists, must be with much weaker dipoles than those associated with XBPs. In examining magnetograms which are displayed to bring up the weaker field regions (20-50 G), mixed polarity small scale features appear everywhere in the quiet Sun. The Kitt Peak magnetograph data is from hours before the rocket flight. We would need to obtain truly simultaneous data and, more importantly, to develop an objective criterion to claim an association with a unique dipole out of those present ubiquitously.

We also find a greater number of C IV events than we would have expected from the results of a disk survey undertaken on the Spacelab 2 flight of the HRTS payload (Cook et al. 1987). Because of the spatial distribution of the C

IV events, we are lead to interpret the X-ray dark lanes as regions of enhanced C IV population. However, this interpretation must be weighed against the possibility that the detection threshold was extended during the HRTS V flight because the spatial resolution of the data is better than that from the Spacelab 2 flight. A resolution of this question must await an increase in the set of coordinated X-ray images and EUV spectra through additional rocket flights or an orbital mission.

We have also determined the transition region spectral features which do correspond with the coronal XBPs. These were found to be larger, brighter structures in C IV than the high velocity events, with a complex velocity structure which, however, did not reach the 100 km s^{-1} velocities seen in the C IV events. Figure 4 shows the HRTS C IV feature corresponding to the prominent XBP at the right side of the raster pattern, toward Sun center. Two consecutive raster steps are illustrated. The XBP covers a raster width approximately equal to its length along the slit, and is seen in both raster steps. A prominent C IV energetic event is also seen in one raster step, but is not present on the step just 2 arc sec away. As with the He I 10830 A dark points (see Fig. 3), we also see C IV spectral features, no different than those corresponding to XBPs, which do not have an XBP corresponding X-ray feature. In the cases both of He I 10830 A dark points and the HRTS transition region C IV observations, only a fraction of all similar events are heated to temperatures where an X-ray signature is also produced.

VI. FUTURE OBSERVING PROGRAMS

The bright point campaign provides an example for the type of collaborative programs which might be attempted during the solar maximum period 1989-1991.

Although there were certainly logistical problems in coordinating multiple sounding rocket launches and simultaneous ground-based observations, the scientific return is more than correspondingly greater. Further, simultaneous observations from all levels of the solar atmosphere continues to be shown as an essential approach to obtain new insight into solar phenomena and must form the backbone of any future orbital solar observatory.

REFERENCES

Brueckner, G.E., and Bartoe, J.-D.F. 1983, Ap. J., 272, 329.

Brueckner, G.E., Bartoe, J.-D.F., Cook, J.W., Dere, K.P., and Socker, D.G., 1986, Adv. Space Res., 6, 263.

Cook. J.W., Bartoe, J.-D.F., Brueckner, G.E., Dere, K.P., Recely, F., Martin, S., and Zirin, H. 1988, B.A.A.S., 20, 722.

Cook, J.W., Brueckner, G.E., and Bartoe, J.-D.F. 1983, Ap. J. Lett., 270, L89.

Cook, J.W., Lund, P.A., Bartoe, J.-D.F., Brueckner,G.E., Dere, K.P., and Socker, G.D. 1987, Fifth Cambridge Workshop on Cool Stars, Stellar Systems, and the Sun, ed. J.L. Linsky and R.E. Stencel (Springer-Verlag), 150.

Martin, S.F., and Harvey, K.L. 1979, Solar Phys., 64, 93.

Moses, J.D., Bartoe, J.-D.F., Brueckner, G.E., Cook, J.W., Dere, K.P., Davis, J.M., and Webb, D. 1988, B.A.A.S., 20, 722.

Moses, D., Schueller, R., Waljeski, K., and Davis, J.M., 1989, SPIE 1159.

Vaiana, G.S., Krieger, A.S., and Timothy, A.F. 1973, Solar Phys. 32, 81.

Vernazza, Avrett, and Loeser 1976, Ap. J. Suppl., 30, 1.

Webb, D.F., and Moses, J.D. 1988, Adv. Space Res., ___, .

FIGURE CAPTIONS

Figure 1. Full disk soft X-ray photographic images used in the Collaborative Bright Point Observing Campaign. Top: 15 August 1987 image, 30 second exposure with organic filter. Bottom: 11 December 1987 image, 60 second exposure with organic filter.

Figure 2. The section of the solar disk containing the HRTS field. North at top, east at left. The map of sites of C IV energetic events is superposed on a HRTS 1600 A spectroheliogram, and the AS&E X-ray, Kitt Peak magnetograph, and Kitt Peak He I 10830 A images.

Figure 3. Top: XBP and He I corresponding dark point compared to Kitt Peak magnetogram of the corresponding dipole from the day before, hours before flight, hours after flight, and the following day. Bottom: Comparison of X-ray image and He I 10830 A image, showing one He I dark point with an XBP corresponding to it, while a second similar He I dark point has no such XBP counterpart.

Figure 4. HRTS slit spectra of C IV 1548 A and 1550 A from two consecutive steps (24 and 25) of the third HRTS raster. The steps are 2 arc sec apart. The C IV counterpart to an XBP is shown, together with a C IV energetic event visible only in Step 25.

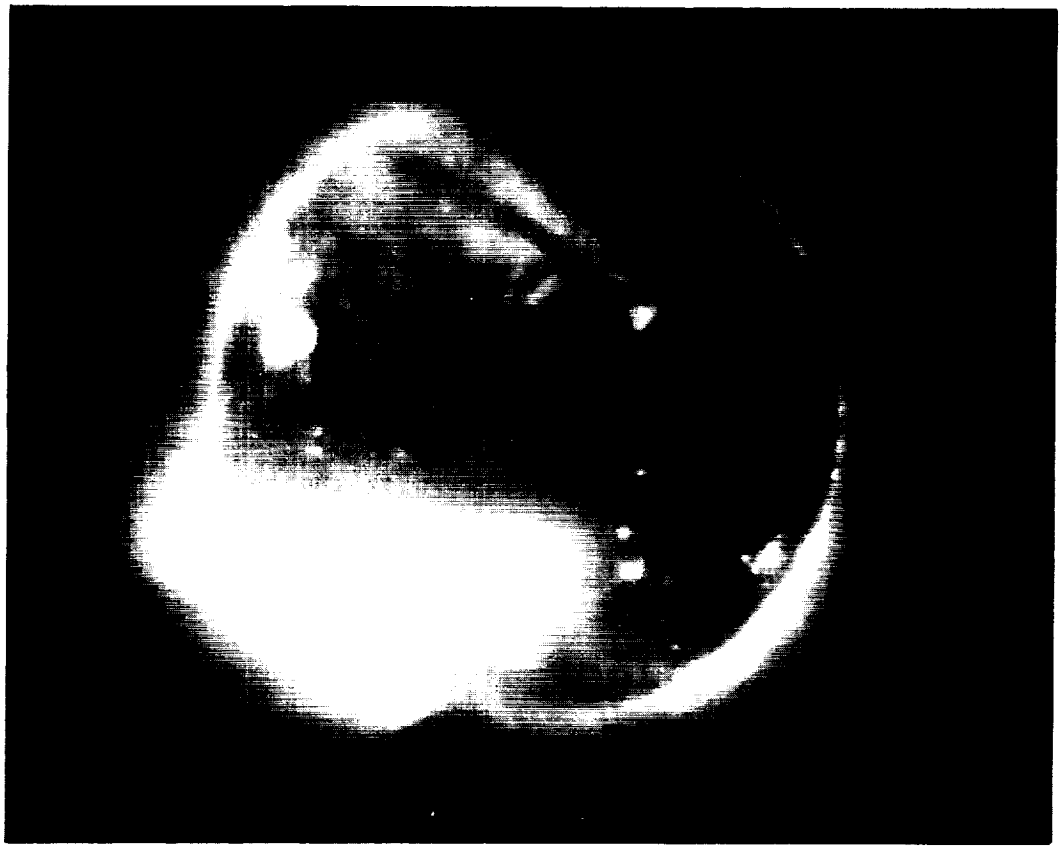

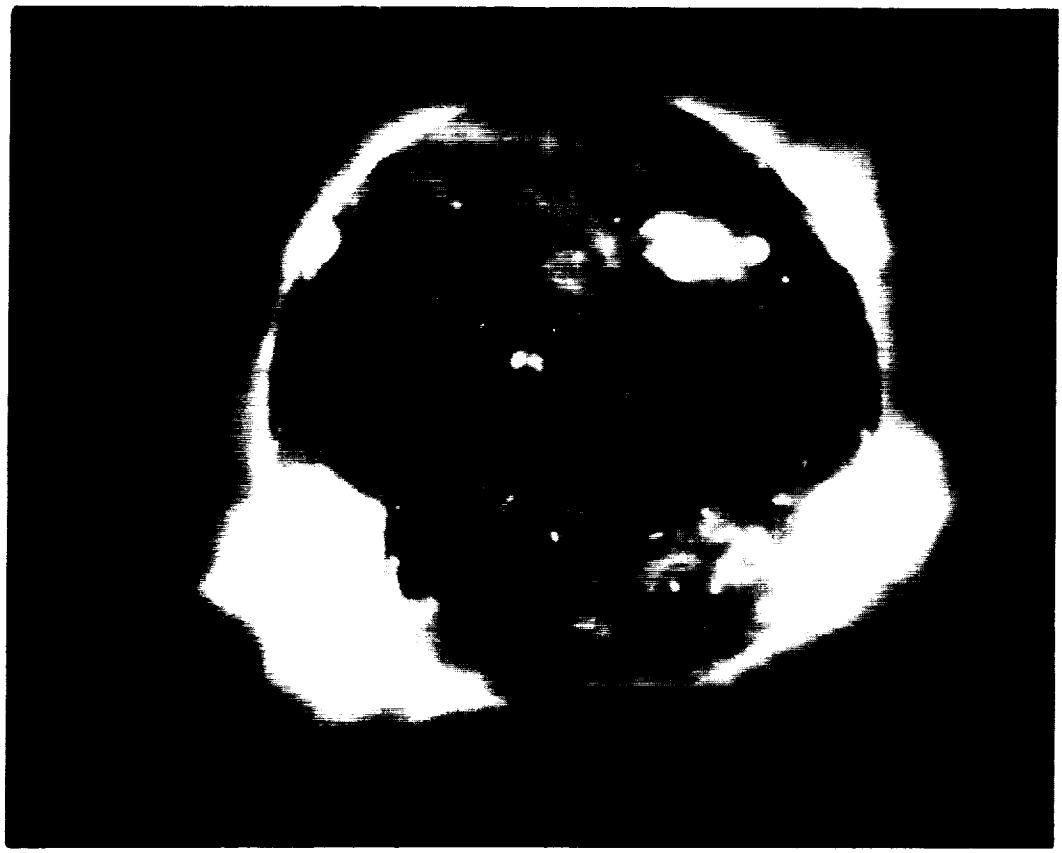

ORIGINAL PAGE
BLACK AND WHITE PHOTOGRAPH

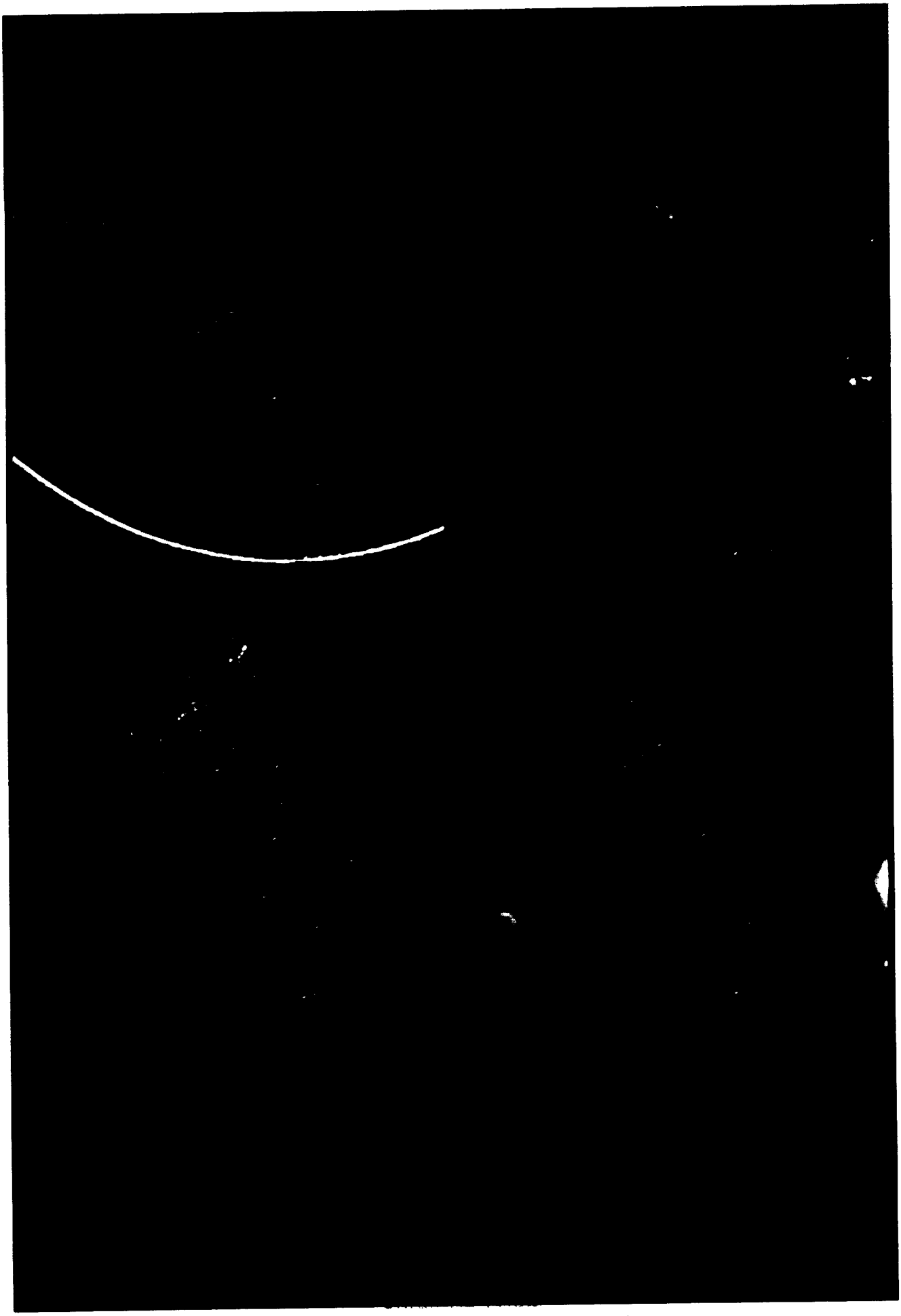

BLACK AND WHITE PHOTOGRAPH

ORIGINAL PAGE
BLACK AND WHITE PHOTOGRAPH

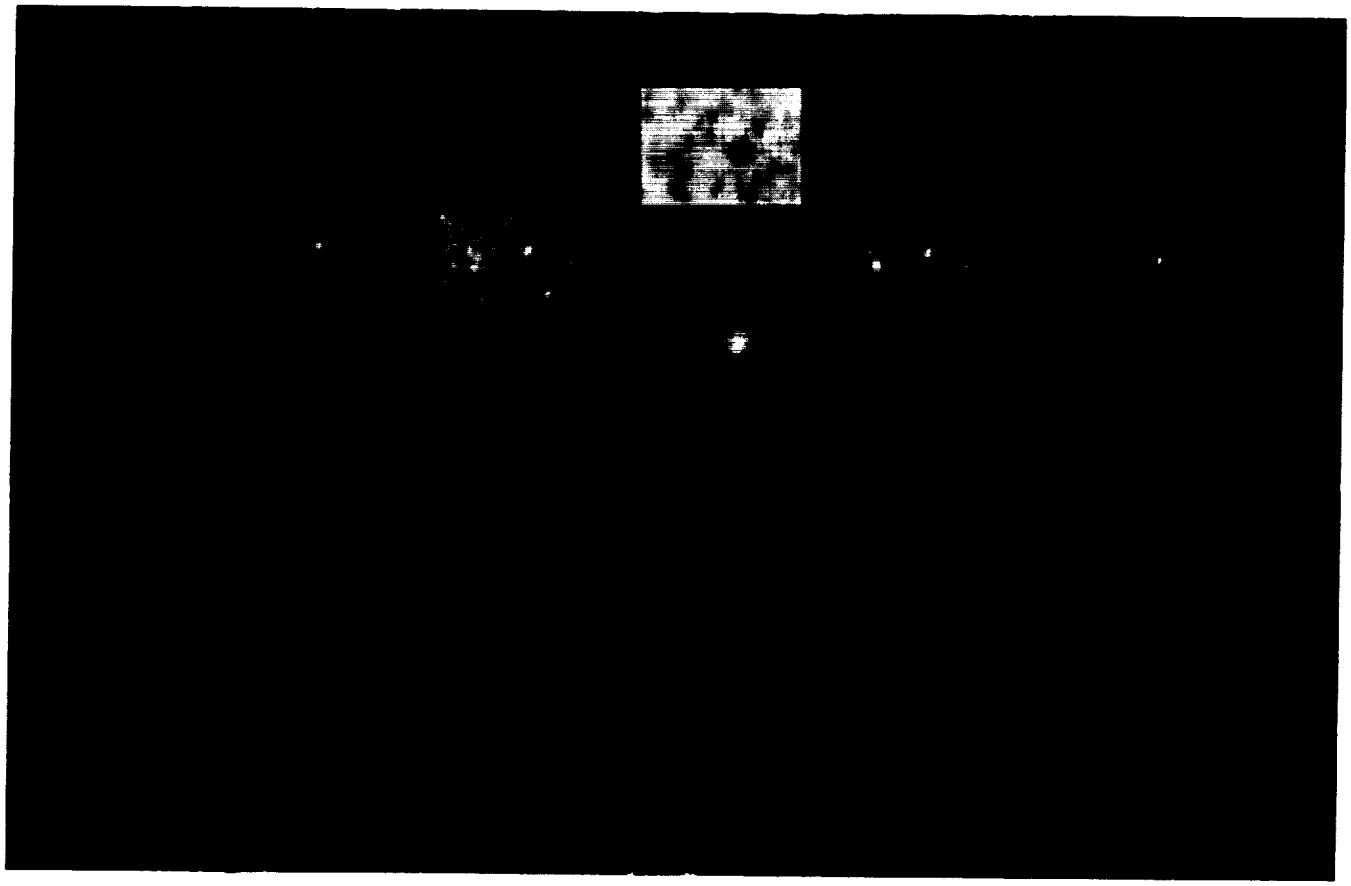

ORIGINAL PAGE
BLACK AND WHITE PHOTOGRAPH